proceedings

MDPI

Proceedings

Source apportionment of atmospheric deposition species in an agricultural Brazilian region using Positive Matrix Factorization†

Jaqueline Natiele Pereira [1], Adalgiza Fornaro[2], Marcelo Vieira-Filho[1]*,

[1] Departamento de Engenharia Ambiental (DAM), Universidade Federal de Lavras (UFLA), Lavras, Minas Gerais, Brazil; jaqueline.pereira@estudante.ufla.br; marcelo.filho@ufla.br.
[2] Instituto de Astronomia, Geofísica e Ciências Atmosféricas (IAG), Departamento de Ciências Atmosféricas (DCA), Universidade de São Paulo (USP), São Paulo, Brazil; adalgiza.fornaro@iag.usp.br.
* Correspondence: marcelo.filho@ufla.br; Tel.: +55 (35) 3829-1666.
† Lavras, Minas Gerais, Brazil. July 2021.

Abstract: We investigated the influence of natural and anthropogenic sources on bulk atmospheric deposition chemistry, from November 2017 until October 2019, in a Brazilian agricultural area. The pH mean value was 5.99 (5.52 – 8.46) and most deposition samples (~98%) were alkaline (pH > 5.60). We identified Ca^{2+} as the predominant specie accounting for 33% of the total ionic species distribution, and as the mainly precursors of atmospheric acidity neutralization (Neutralization Factor = 6.63). PMF analysis resulted in four factors, which demonstrated the influence of anthropogenic and natural sources, such as fertilizer application and production, marine intrusion / biomass burning and biogenic emissions, and revealed the importance of atmospheric neutralization processes.

Keywords: Atmospheric Deposition; Source apportionment; Agricultural region; PMF; Brazil

Pereira, J. N.; Fornaro, A.; Vieira-Filho, M. Source apportionment of atmospheric deposition species in an agricultural Brazilian region using Positive Matrix Factorization. *Proceedings* **2021**, *65*, x. https://doi.org/10.3390/xxxxx
Received: date
Accepted: date
Published: date

Publisher's Note: MDPI stays neutral with regard to jurisdictional claims in published maps and institutional affiliations.

Copyright: © 2021 by the authors. Submitted for possible open access publication under the terms and conditions of the Creative Commons Attribution (CC BY) license (http://creativecommons.org/licenses/by/4.0/).

1. Introduction

Because of rapid economic development, increased energy consumption, anthropogenic activities and industrialization in the last centuries, was inevitable the atmospheric accumulation of several gases and aerosols [1]. These mentioned pollutants are removed from the atmosphere to Earth's surface mainly by bulk deposition processes, which encompasses wet (in-cloud and below-cloud scavenging processes) and dry deposition (scavenging processes in precipitation absence) [2]. Therefore, owing to atmospheric deposition, nutrients and pollutants may entry into terrestrial and aquatic ecosystems causing significant impacts, such as eutrophication and soil acidity [3].

Atmospheric deposition chemistry has been widely studied in many areas worldwide, since provide useful information that feeds several receptor models to identify anthropogenic and natural source apportionment [4–7]. Broadly, natural origin is relation to marine salt and soil dust, while anthropogenic origins are mainly fossil fuel combustion, industrial processes and agricultural production [8].

Moreda-Piñeiro et al. [9] assessed rainwater samples in Spain and reported that Cl^-, Na^+ and Mg^{2+} were linked to sea-salt origin, while SO_4^{2-} and Ca^{2+} were released from a terrestrial crustal source. Also in this study, NH_4^+ and NO_3^- were mainly attributed to agricultural activity.

Statistical techniques, such as Factor Analysis (FA), Principal Component Analysis (PCA), Chemical Mass Balance (CMB) and Positive Matrix Factorization (PMF), have been employed as receptor models for identification of the main pollutants sources [10–12]. However, PMF is commonly applied to airborne particles and atmospheric gases [13,14] and scarcely to bulk atmospheric deposition, due to complexity of its process [15].

Considering the absence of an established network for routinely monitoring wet and dry deposition in Brazil [16], a study was carried out in the Southern Region of Minas Gerais, which is an important economic region responsible for 21.8% of agricultural commodities (mainly from coffee producing regions), and also accounts for about 12% of the state's Gross Domestic Product [17]. In this sense, we investigated the influence of natural and anthropogenic sources on bulk atmospheric deposition chemistry in the Lavras city, South of Minas Gerais, using PMF.

2. Material and Methods

2.1. Study Area

Lavras is located in the Southern Minas Gerais state (21° 13' 45,3"S and 44° 58' 32,4"W), Brazil, 241 km from the Atlantic Ocean (in a straight line), with an area of 564.744 km², altitude of 919 m (Fig.1) and a population of the 102,728 inhabitants [18]. Lavras soil is predominantly classified as Dystrophic Red-Yellow Oxisol (RYOd1) and Eutrophic Red-Yellow Argisol (RYAe12). RYOd1 soils are suitable for tillage but are naturally acids [19]. Therefore, the liming process is common, in which lime is applied to correct soil acidity for agricultural purposes. In this sense, Lavras generally is known for its agricultural production, since has about 19% (107 km²) of its total area associated with agricultural activities, mainly coffee production [20].

Lavras also undergo influence of several anthropogenic activities including transport, farming, biomass burning and industrial activities such as agroindustrial, limestone mining and cement plants [17]. The vehicular fleet has about 50 thousand light-duty vehicles, corresponding to 54% of automobiles and 26% of motorcycles. Moreover, vehicle fleet was on average 15 years old, where 62% of passenger cars were produced before 2010 and only 14% before 1990 [21].

Regarding weather conditions, the city presents climatological (1981-2010) mean annual temperature of 20.3 °C, with minimum (16.9 °C) values in July and maximum (22.8 °C) in February. The annual rainfall of 1461.8 mm is mainly

concentrated in two well defined periods: (i) rainy season from October to March (covering 85% of total rainfall); and (ii) a dry one from April to September [22].

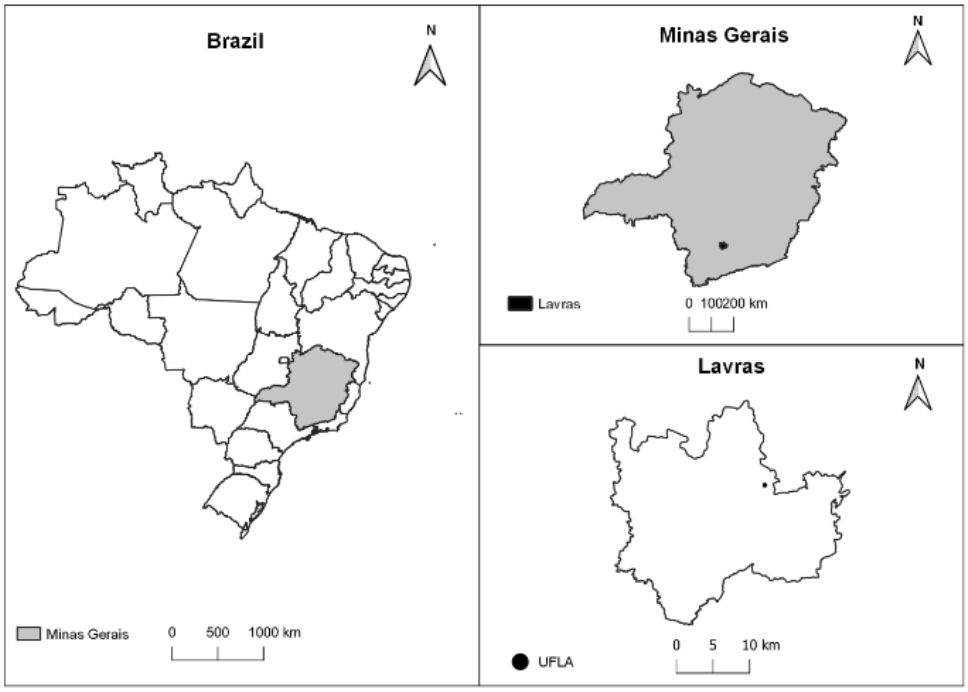

Figure 1. Geographical location of sampling site (UFLA) in Lavras city, Southern Minas Gerais state, Brazil

2.2. Sampling and Sample Analysis

A total of 65 bulk deposition samples were collected at *Universidade Federal de Lavras (UFLA)* campus in Lavras city (Fig. 1), between November 2017 and October 2019. We using a handmade sampler composed of a high-density polyethylene bucket (NALGON) of 10L with a collecting area of 439 cm^2, protected by a sun-protective PVC structure and covered with a nylon mesh. In order to follow GAW´s sampling procedures, we kept the sampler 1.5 m above the ground and clean it with deionized water (18 MΩ) [23]. Highlighted that for dry atmospheric only samples, a 50 mL of deionized water was added in order to analyze soluble species.

Samples were collected at intervals of about 7 days and after each collect were divided into two parts. In a fraction we measure pH using pHmeter (AKSO AK model 151), calibrated with buffer solutions (pH 4.0 and 7.0). The other sample aliquot was filtered with a 0.22 μm diameter membrane (Millex), stored in pre-cleaned polyethylene bottles kept at -18 °C prior to ion chromatography (IC) analysis (Metrohm model 851) with anionic column (Metrosep ASupp5 - 250 mm x 4 mm) and cationic column (Metrosep C2 150 - 150 x 4 mm). Analytical quantification was performed using an external calibration curve from the standards concentrations for each ion. The species quantified by IC were calcium (Ca^{2+}), ammonium (NH_4^+), magnesium (Mg^{2+}), sodium (Na^+), potassium (K^+), nitrate (NO_3^-), chloride (Cl^-

), sulfate (SO_4^{2-}), fluoride (F^-), formate (CHO_2^-), acetate ($C_2H_3O_2^-$) and oxalate ($C_2O_4^{2-}$), all presenting detection limits (DL) lower than 0.8 $\mu molL^{-1}$. Also, blank samples analysis were carried out through the sampling campaign.

2.3. Data Analysis

Data processing was performed by programming in R language, specifically the functions contained in the stats and ggplot2 packages [24,25].

2.3.1. Samples Validation

The internal consistency of the entire data set was analyzed through Cooperative Programme for Monitoring and Evaluation of Long-Range Transmission of Air Pollutants in Europe (EMEP) guidelines for rainwater samples validation [23]. This method is based in the equations 1, 2 and 3:

$$IS = \sum_{cations} C_i + \sum_{anions} C_i \quad (1)$$

$$ID = \sum_{cations} C_i - \sum_{anions} C_i \quad (2)$$

$$IB = (ID/IS) * 10^2 \quad (3)$$

Where C_i is the concentration of ion type i in a specific sample, expressed in μeqL^{-1}. IS is the sum of all ion concentrations and ID is the difference between the sum of the cation concentrations and the sum of the anion concentrations. Both IS and ID are expressed in μeqL^{-1}. The ion balance, IB, expresses the difference, ID, in percent of the sum of all concentrations, IS. Apart from the equations, the samples pH values were also considered in this validation process, a critical value of 5.5 was used, moreover specific details are described elsewhere [23,26].

2.3.2. Non-measure Species Estimate

We estimate bicarbonate (HCO_3^-) concentrations from theoretical relationship between pH and HCO_3^- (Eq. 4), and for carbonate (CO_3^{2-}) we considered the same concentration of Ca^{2+} (WMO, 2004), since no direct method was applied for measuring these species.

$$[HCO_3^-] = 5.1/10^{6-pH} \quad (4)$$

2.3.3. Volume Weighted Mean

The volume weighted mean (VWM) was expressed through the relationship between the sum of the concentrations product of each species (X_i) found in the n samples by the respective volume (V_i) and the sum of all the samples volumes according to the equation 5 [27]. For dry atmospheric deposition samples, in which we added 50 mL of deionized water due to precipitation absence, we considered that volume for calculations.

$$VWM = \frac{\sum_{i=1}^{n}(X_i * V_i)}{\sum_{i=1}^{n} V_i} \quad (5)$$

2.3.4. Neutralization Factor

The neutralization factor (NF) or index was calculated to assess the role of crustal components (Ca^{2+} and Mg^{2+}) and NH_4^+ on the neutralization of rainwater acidity due to the presence of NO_3^- and SO_4^{2-}, using the equation 6 adapted from Huang et al. and Qiao et al. [28,29]:

$$NF_X = \frac{[X]}{[NO_3^-] + [SO_4^{2-}]} \quad (6)$$

Where X is the cation of interest and all the concentrations were used in μeqL^{-1}.

2.3.5. Positive Matrix Factorization (PMF)

In order to identify sources of pollutants and their relative contributions we using the software Positive Matrix Factorization (PMF, version 5.0) made available by United States Environmental Protection Agency, which consists of a mathematical receptor model [30].

In general, a receptor model aims to solve the chemical mass balance between the species measured concentrations and the sources profiles [31]. In this sense, the PMF model decomposes a matrix of sample data into one matrix of factor contributions (G) and other of factor profiles (F). Then, for a data matrix X of n samples by m chemical species, the model will identify the number of factors p, the species profile f_k of each factor k, and the amount of mass g_k contributed by each factor k to each individual sample, according to Eq. 7:

$$X_{ij} = \sum_{k=1}^{p} g_{ik} f_{kj} + e_{ij} \quad (7)$$

Where e_{ij} is the residual, i and j are the rows and columns of X.

The factor contributions and profiles are derived by the PMF model minimizing the Q function (Eq.8), with non-negativity constraints, i.e. $g_{ik} > 0$ and $f_{kj} > 0$ [32,33].

$$Q = \sum_{i=1}^{n} \sum_{j=1}^{m} \left[\frac{X_{ij} - \sum_{k=1}^{p} g_{ik} f_{kj}}{u_{ij}} \right]^2 (8)$$

Where u_{ij} are variable uncertainties, which allowing each data value to be individually weighted. These variable uncertainties (u_{ij}) for data with values below and above the DL were calculated according to equations 9 and 10, respectively [31,34].

$$u_{ij} = 5\,\overline{DL}_{ij}/6 \quad (9)$$

$$u_{ij} = \sqrt{(Error\ Fraction * Concentração_{ij})^2 + (0.5 * DL_{ij})^2} \quad (10)$$

Where the error fraction was estimated at 10% [35].

The quality of data was assessing based on the signal to noise ratio (S/N), which characterize species as strong when S/N > 2.0 and as weak in the cases that S/N ranged from 0.2 to 2.0. The species with S/N < 0.2 or values below DL greater than 50% were categorized as bad in quality and were excluded from the PMF analysis [36].

3. Results and Discussion

3.1. Samples Validation

The pH values for the whole data set (n = 65) ranged from 5.34 to 8.46 with average of 5.89. Given the samples alkaline behavior, quality assurance and quality control (QA/QC) were verified applying the criteria from EMEP. Following the QA/QC, among the 65 atmospheric deposition events, 7 were invalid, 3 valid and 55 valid and flagged (Fig.2a). Only seven invalid samples were rejected and, thereby, we considered a new data set (n = 58) in the following discussion.

In order to verify the electroneutrality principle, a sum of anions *versus* cations plot was depicted in Fig.2b, in units of μeqL^{-1}. In general, we observed a good and statistical significant linear fit (R^2 = 0.80 and p-value < 0.01) for the data set. In addition, the sum of cations was greater than the sum of anions, since the fitted line slope (value of 0.42 – Fig.2b) was lower than the unity. The anions deficit was reasonable in samples with pH values ranging from 5.5 to 6.0 [26] and which could have been attributed to the lack of measurements of carbonate and bicarbonate concentration [37–39]. In order to identify the carbonate deficit, an estimative of these species was carried out (WMO, 2004) and a new sum of cations *versus* anions plot was constructed (Fig.2c). It is noteworthy that the new angular coefficient presented a value of 1.09, which was closer to 1, with determination coefficient of 96% (p-value < 0.01). The bicarbonate estimation produced a poor linear adjustment (slope = 0.32 and R^2 = 0.04 with p-value 0.07) and therefore we considered only the presence of carbonate in the bulk atmospheric deposition samples.

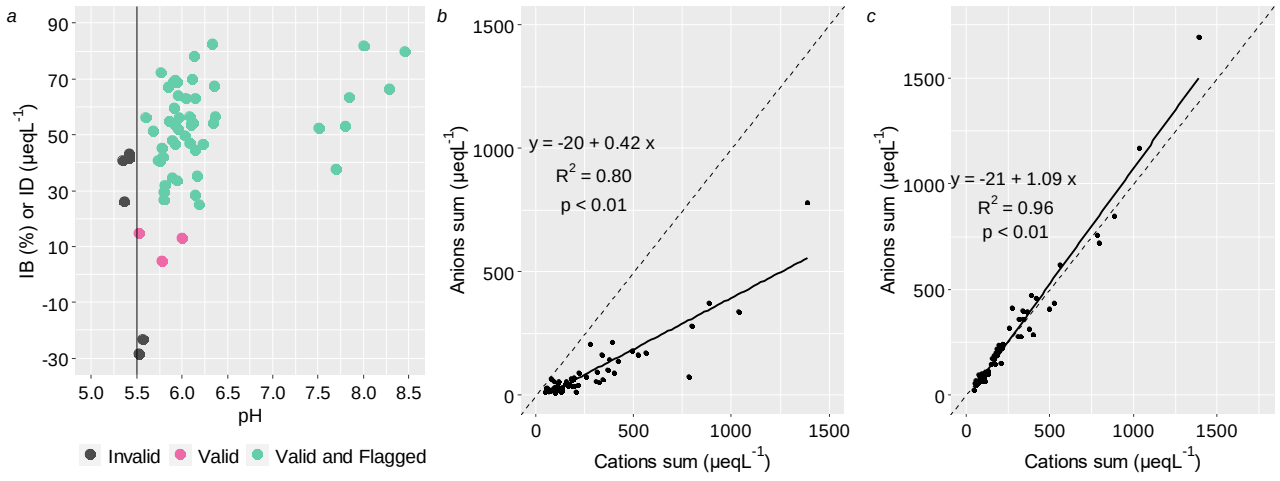

Figure 2. Ionic balance in bulk atmospheric deposition of Lavras city: (a) samples validation criteria from EMEP (n = 66) and the reference line represent a critical pH (5.5) value; (b) anions sum *vs*. cations sum (n = 58) and the dashed line represent the ideal slope of 1; (c) anions sum *vs.* cations sum considering the carbonate estimate (n = 58) and the dashed line represent the ideal slope of 1. Sampling period was between November 2017 and October 2019

3.2. pH Variation

The mean pH value for validated samples (n = 58) was 5.99 (5.52–8.46) (Fig.3). Once 5.60 represents the pH value resulting from the equilibrium between atmospheric CO_2 and pure water and is also used as a limit for acid rain [40–42], our results suggests inputs of alkaline species into the atmosphere (98% of samples with pH > 5.60). This behavior is in agreement with other studies carried out in Brazil, such as those performed in Campo Bom, Rio Grande do Sul [35] and in Juiz de Fora, Minas Gerais [43], in which the authors associated high pH values to inputs of crustal aerosols, containing large fraction of carbonate and bicarbonate, in the atmosphere deposition.

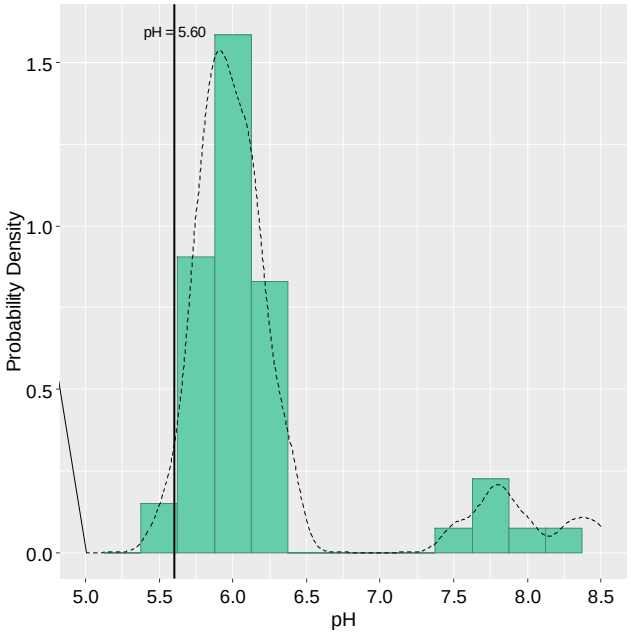

Figure. 3 Histogram of the pH values of the 58 bulk atmospheric deposition samples in Lavras city, from November 2017 until October 2019. The vertical line refers to critical value for rainwater acidity classification (pH = 5.60) and the dotted line represents the probability density curve

3.3. Ionic Composition

Concentration of major ions in $\mu molL^{-1}$ is illustrated in Fig 4. Among all cations, Ca^{2+} was the specie with greater variability (6.82 – 455 $\mu molL^{-1}$), following by Na^{2+} (0.03 – 179 $\mu molL^{-1}$). Regarding anionic species, Cl^- was the dominant compound with the largest variability (0.06 – 346 $\mu molL^{-1}$), following by NO_3^- (0.11 – 213 $\mu molL^{-1}$). The organic anions (acetate, formate and oxalate) along with F^- and H^+ presented the smallest variability, since that all these ions had concentrations below than 50 $\mu molL^{-1}$.

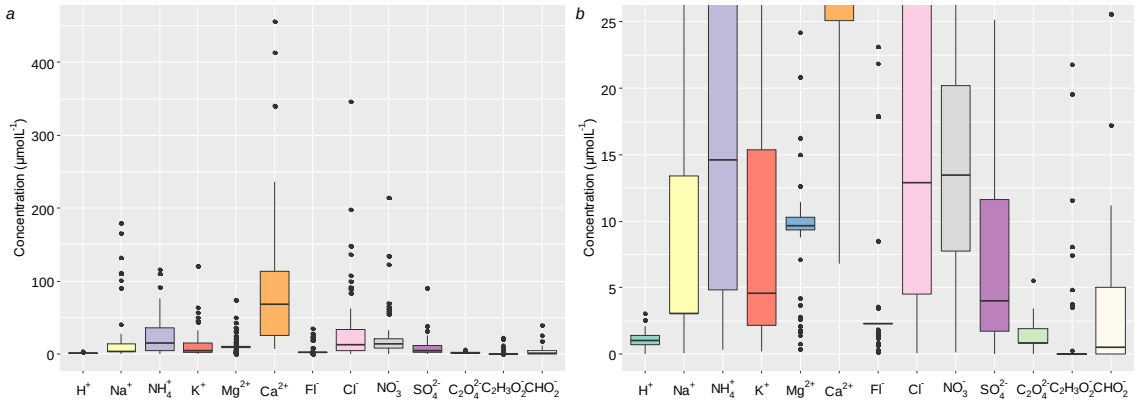

Figure. 4 Box and whisker plots for the ions identified and quantified in bulk atmospheric deposition in Lavras, from November 2017 until October 2019. Horizontal lines in the box represent the 25th, 50th and 75th percentile values. (a) Depicts all the ionic concentrations; and (b) magnifies the species with concentrations between 0 and 25 μmolL^{-1}

VWM concentrations were more amenable for comparisons and were calculated for all measured ions. For the whole sampling campaign, the ions profile in VWM (molar unit) may be described in the following order: Ca^{2+} (45.7) > Cl^- (19.1) > Na^+ (16.6) > NH_4^+ (14.4) > Mg^{2+} (12.8) > NO_3^- (9.46) > K^+ (5.48) > F^- (4.00) > SO_4^{2-} (3.88) > HCO_2^- (1.92) > $C_2H_3O_2^-$ (1.41) > $C_2O_4^{2-}$ (1.26) > H^+ (0.77) μmolL^{-1}. We identified Ca^{2+} as the most predominant specie accounting for 33%, which coupled with Na^+ and NH_4^+ represents 56% of the total ionic species distribution. Similar patterns were observed in Mbita, East Africa, which also is characterized as a tropical agricultural area [44]. It is also valuable mentioning that Cl^- was the second largest ion, contributing with 13% of the total VWM concentration.

3.4. Neutralization Factor

We calculated the NF index in order to assess the influence of alkaline species in atmospheric samples. The $NF_{Ca^{2+}}$ ranged between 0.99 and 29.6 while $NF_{Mg^{2+}}$ and NF_{NH4^+} varied from 0.05 to 11.0 and from 0.01 to 7.14, respectively. Considering the mean values for all study period, the most important neutralizing agent of sulfuric and nitric acids was Ca^{2+} (NF = 6.63), followed by Mg^{2+} (NF =1.54) and NH_4^+ (NF = 1.11), which may be considered negligible. The role of Ca^{2+} as a dominant neutralization cation is reasonable since the calcium presented the highest VWM for the entire period studied. On the other hand, Mg^{2+} contributed more than NH_4^+ for samples neutralization although NH_4^+ has presented higher VWM concentration, suggesting that this neutralization proxy is better suited for assessing the major chemical species interactions in rich alkaline atmosphere such as in Lavras city. Highlighted that Ca^{2+} precursor, as calcium carbonate, was sufficient to neutralize the major atmospheric acids, since most samples (n = 57 ~ 98%) showed NF higher than neutrality (NF = 1). This pattern is in agreement with the pH values found.

Similar phenomena have been observed in a number of previous studies in Brazil [35,45] and worldwide [46–50]. In contrast, some studies have been reporting the predominance of NH_4^+ [51,52] and Mg^{2+} [6] in the atmospheric neutralization process.

3.5. Source Identification Based on PMF Results

PMF is adopted to quantitatively analyze the emission sources of the measured ionic species. According to S/N ratio, all species were categorized as strong, except the acetate that was classified as weak (S/N = 1.5). However, due to large amount of data below of DL (> 50%), acetate and formate were classified as bad and excluded from the analysis. The PMF model was run 20 times with a seed of 76 random starting points and a number of factors from 3 to 6 were assessed to get the optimal number of factors. The stability and reliability of the output were checked according to following parameters: Q value, parameters of linear regression between predicted and observed concentrations, frequency distributions of the scaled residuals, G-space plots and the physical meaning of the factor profiles. Based on the evaluation of these criteria, we identify that four factors were physically reasonable and could represent the major sources in the study region (Fig. 5).

The first factor identified presented high loading values for NH_4^+ (85%), Mg^{2+} (70%) and F^- (64%). The presence of F^- is associated with HF gas emission, mostly from the productions of steel, electrolytic aluminum and phosphorus fertilizers [53,54]. Mg^{2+} is originated naturally from the marine aerosols and/or crustal particles (Zhou et al. 2019), and its anthropogenic sources can be associated to cement industries and fertilizers production. Regarding NH_4^+, can be directly attributed to an input of NH_3 in the atmosphere, mainly due to farming and nitrogen fertilizers production and application [52]. This profile corroborates with the agricultural background of the study region, where an average nitrogen and phosphor synthetic fertilizers application rate was estimated in 194 $kgha^{-1}$ [56]. In addition, there are several agroindustrials inside the county air basin. Thus, this factor was categorized as *fertilizer application and production*.

The second factor, named *atmospheric neutralization processes*, was represented by Ca^{2+} (83%), NO_3^- (71%) and SO_4^- (70%). These species are involved in neutralizing atmospheric processes, since that $CaCO_3$ is an alkaline specie that neutralize the major atmospheric acids (H_2SO_4 and HNO_3). Highlighted that cement manufacturing and limestone mining were considered the two major sources of Ca^{2+} to the atmosphere in the study area. Although NO_3^- and SO_4^- have been related to the large emissions of SO_2 and NO_x from the combustion of fossil fuel in large urban areas [39], researches carried out in agricultural areas in California, United States, associated these species with agricultural soil emissions [57], which is reasonable with our study.

Factor 3, was loaded with Na^+ (80%), K^+ (67%) and Cl^- (78%). These species generally originate from sea-salt, crustal aerosols and biomass burning [58]. In the present study, the Cl^-/Na^+ ratio was 1.15, which was similar to oceanic ratio ($Cl^-/Na^+ = 1.17$), indicating marine sources intrusion. However, the K^+/Na^+ ratio was 0.33, which was higher than oceanic ratio ($K^+/Na^+ = 0.022$), suggesting a large excess of K^+ and, therefore, suggesting an additional source of potassium compounds in Lavras city, as biomass burning. Because of the ambiguity of sources in this factor, was characterized as *marine intrusion / biomass burning*.

Factor 4 was categorized as *biogenic emissions* due to high loaded for oxalate (93%). Organic acids in the atmosphere in large urban areas originate from motor vehicle emissions, fossil fuel combustion and photochemical reactions. However, in rural areas biogenic emissions, such as vegetation release and the burning of biomass, are more important sources of organic acids [59].

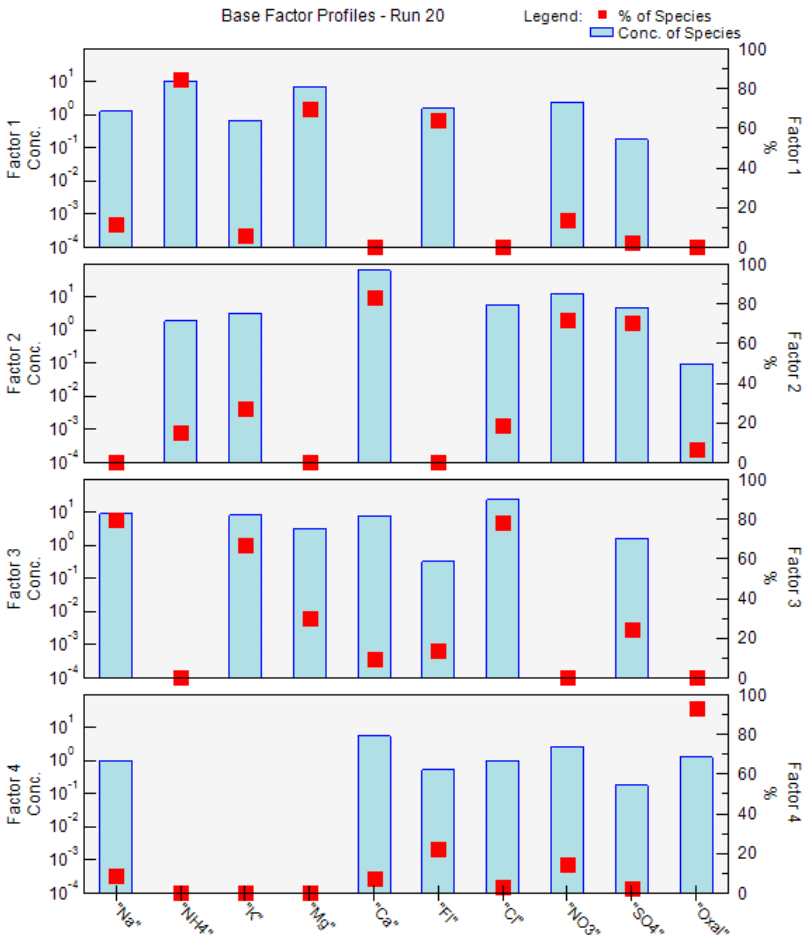

Figure. 5 Source profiles extracted by EPA PMF 5.0 model from bulk deposition samples collected in Lavras, in the period between November 2017 and October 2019

4. Conclusions

We assessed bulk atmospheric deposition in a Brazilian agricultural region and observed that pH mean was 5.99 and most deposition samples (~98%) were alkaline (pH > 5.60). In addition, the most important neutralizing agent of sulfuric and nitric acids was Ca2+ precursors (NF = 6.63). This process was corroborated by the higher abundance of Ca^{2+} (33%) among all ions measured. The PMF analysis resulted in four factors, which demonstrated the influence of anthropogenic and natural sources, such as fertilizer application and production, marine intrusion / biomass burning and biogenic emissions, and revealed the importance of atmospheric neutralization processes.

The atmospheric deposition systemic analysis allowed to monitor and evaluate the chemical transformation processes, reaction routes and the identification of the polluting sources. From that, it is possible to develop emission reduction strategies, as effectively done in the previous decades for acid rain. Given this perspective, our findings are useful to understand the majority atmospheric species sources in the Southern Minas Gerais, Brazil.

Author Contributions: Conceptualization, M.V.F., J.N.P and A.F.; methodology, M.V.F., J.N.P and A.F.; software, J.N.P; data curation, M.V.F., J.N.P.; writing—original draft preparation, M.V.F., J.N.P; writing—review and editing, M.V.F., J.N.P, A.F.; supervision, M.V.F.; project administration, M.V.F.; funding acquisition, M.V.F. and A.F.. All authors have read and agreed to the published version of the manuscript.

Institutional Review Board Statement: Not applicable.

Informed Consent Statement: Not applicable.

Acknowledgments: The authors thank to Coordenação de Aperfeiçoamento de Pessoal de Nível Superior (CAPES) and Fundação de Amparo à Pesquisa do Estado de Minas Gerais (Fapemig) for the Graduate and Undergraduate Scholarships. Special thanks go to "Laboratório de Processos Atmosféricos da Universidade de São Paulo (LAPAt-IAG-USP)" for the facilities and equipments used in this study.

Conflicts of Interest: The authors declare no conflict of interest.

References

1. Kamani, H.; Hoseini, M. Study of trace elements in wet atmospheric precipitation in Tehran , Iran. **2014**, doi:10.1007/s10661-014-3759-9.
2. Araujo, T.G.; Souza, M.F.L.; De Mello, W.Z.; Da Silva, D.M.L. Bulk Atmospheric Deposition of Major Ions and Dissolved Organic Nitrogen in the Lower Course of a Tropical River Basin, Southern Bahia, Brazil. *J. Braz. Chem. Soc.* **2015**, *26*, 1692–1701, doi:10.5935/0103-5053.20150143.
3. Duan, L.; Chen, X.; Ma, X.; Zhao, B.; Larssen, T.; Wang, S.; Ye, Z. Atmospheric S and N deposition relates to increasing riverine transport of S and N in southwest China: Implications for soil acidification. *Environ. Pollut.* **2016**, *218*, 1191–1199, doi:10.1016/j.envpol.2016.08.075.
4. Sun, X.; Wang, Y.; Li, H.; Yang, X.; Sun, L.; Wang, X.; Wang, T.; Wang, W. Organic acids in cloud water and rainwater at a mountain site in acid rain areas of South China. *Environ. Sci. Pollut. Res.* **2016**, *23*, 9529–9539, doi:10.1007/s11356-016-6038-1.
5. Zhou, X.; Xu, Z.; Liu, W.; Wu, Y.; Zhao, T.; Jiang, H.; Zhang, X.; Zhang, J.; Zhou, L.; Wang, Y. Chemical composition of precipitation in Shenzhen, a coastal mega-city in South China: Influence of urbanization and anthropogenic activities on acidity and ionic composition. *Sci. Total Environ.* **2019**, *662*, 218–226, doi:10.1016/j.scitotenv.2019.01.096.
6. Deusdará, K.R.L.; Forti, M.C.; Borma, L.S.; Menezes, R.S.C.; Lima, J.R.S.; Ometto, J.P.H.B. Rainwater chemistry and bulk atmospheric deposition in a tropical semiarid ecosystem: the Brazilian Caatinga. *J. Atmos. Chem.* **2017**, *74*, 71–85, doi:10.1007/s10874-016-9341-9.
7. Szép, R.; Bodor, Z.; Miklóssy, I.; Niță, I.A.; Oprea, O.A.; Keresztesi, Á. Influence of peat fires on the rainwater chemistry in intra-mountain basins with specific atmospheric circulations (Eastern Carpathians, Romania). *Sci. Total Environ.* **2019**, *647*, 275–289, doi:10.1016/j.scitotenv.2018.07.462.
8. Rastegari Mehr, M.; Keshavarzi, B.; Sorooshian, A. Influence of natural and urban emissions on rainwater chemistry at a southwestern Iran coastal site. *Sci. Total Environ.* **2019**, *668*, doi:10.1016/j.scitotenv.2019.03.082.
9. Moreda-Piñeiro, J.; Alonso-Rodríguez, E.; Moscoso-Pérez, C.; Blanco-Heras, G.; Turnes-Carou, I.; López-Mahía, P.; Muniategui-Lorenzo, S.; Prada-Rodríguez, D. Influence of marine, terrestrial and anthropogenic sources on ionic and metallic composition of rainwater at a suburban site (northwest coast of Spain). *Atmos. Environ.* **2014**, *88*, 30–38, doi:10.1016/j.atmosenv.2014.01.067.
10. Kuzu, S.L.; Saral, A. The effect of meteorological conditions on aerosol size distribution in Istanbul. *Air Qual. Atmos. Heal.* **2017**, *10*, 1029–1038, doi:10.1007/s11869-017-0491-y.
11. Anil, I.; Alagha, O.; Karaca, F. Effects of transport patterns on chemical composition of sequential rain samples: trajectory clustering and principal component analysis approach. *Air Qual. Atmos. Heal.* **2017**, *10*, doi:10.1007/s11869-017-0504-x.
12. Zhang, N.; Cao, J.; He, Y.; Xiao, S. Chemical composition of rainwater at Lijiang on the Southeast Tibetan Plateau: Influences from various air mass sources. *J. Atmos. Chem.* **2014**, *71*, 157–174, doi:10.1007/s10874-014-9288-7.
13. Khan, M.F.; Latif, M.T.; Saw, W.H.; Amil, N.; Nadzir, M.S.M.; Sahani, M.; Tahir, N.M.; Chung, J.X. Fine particulate matter in the tropical environment: Monsoonal effects, source apportionment, and health risk assessment. *Atmos. Chem. Phys.* **2016**, *16*, 597–617, doi:10.5194/acp-16-597-2016.
14. Sofowote, U.M.; Su, Y.; Dabek-Zlotorzynska, E.; Rastogi, A.K.; Brook, J.; Hopke, P.K. Sources and temporal variations of constrained PMF factors obtained from multiple-year receptor modeling of ambient PM2.5 data from five speciation sites in Ontario, Canada. *Atmos. Environ.* **2015**, *108*, 140–150, doi:10.1016/j.atmosenv.2015.02.055.
15. Roy, A.; Chatterjee, A.; Tiwari, S.; Sarkar, C.; Das, S.K.; Ghosh, S.K.; Raha, S. Precipitation chemistry over urban, rural and high altitude Himalayan stations in eastern India. *Atmos. Res.* **2016**, *181*, 44–53, doi:10.1016/j.atmosres.2016.06.005.
16. Lara, L.B.L.S.; Artaxo, P.; Martinelli, L.A.; Victoria, R.L.; Camargo, P.B.; Krusche, A.; Ayers, G.P.; Ferraz, E.S.B.; Ballester, M. V. Chemical composition of rainwater and anthropogenic influences in the Piracicaba River Basin, Southeast Brazil. *Atmos.*

Environ. **2001**, *35*, 4937–4945, doi:10.1016/S1352-2310(01)00198-4.

17. Almeida, G.L.M.D.; Ferreira, E.C. da M.; Mendes, D.J. da S.; Gomes, B.A.B.; Souza, F. do N.; Silva, J. do N.; Dos Santos, S.A.; Teixeira, P.B. *Estudo sobre as regiões de planejamento de Minas Gerais: Sul de Minas Gerais*; Belo Horizonte, 2017;
18. IBGE Cidades e Estados: Lavras Available online: https://cidades.ibge.gov.br/brasil/mg/lavras (accessed on Jun 1, 2019).
19. EMBRAPA *Levantamento de Reconhecimento de Média Intensidade dos Solos da Zona Campos das Vertentes - MG*; 2006;
20. IBGE Produção Agrícola Municipal Available online: https://sidra.ibge.gov.br/Tabela/5457 (accessed on Jun 3, 2021).
21. DENATRAN Frota de Veículos - 2018 Available online: https://infraestrutura.gov.br/component/content/article/115-portal-denatran/8558-frota-de-veiculos-2018.html (accessed on Jun 1, 2019).
22. INMET Normais Climatológicas do Brasil Available online: http://www.inmet.gov.br/portal/index.php?r=clima/normaisClimatologicas (accessed on Sep 15, 2019).
23. WMO *Manual for the Gaw Precipitation Chemistry Programme: Guidelines, Data Quality Objectives and Standard Operating Procedures*; 2004;
24. R Core Team R: A Language and Environment for Statistical Computing 2019.
25. Wickham, H. ggplot2: Elegant Graphics for Data Analysis 2016.
26. Schaug, J.; Semb, A.; Hjellbrekke, A.-G.; Hanssen, J..; Pedersen, A. *Data quality and quality assurance report*; Kjeller, Norway, 1997;
27. Clarke, N.; Žlindra, D.; Ulrich, E.; Mosello, R.; Derome, J.; K, D.; König, N.; Lövblad, G.; Draaijers, G.; Hansen, K.; et al. *Manual on methods and criteria for harmonized sampling, assessment, monitoring and analysis of the effects of air pollution on forests - Part XIV*; Eberswalde, Germany, 2016;
28. Huang, D.Y.; Xu, Y.G.; Peng, P.; Zhang, H.H.; Lan, J.B. Chemical composition and seasonal variation of acid deposition in Guangzhou, South China: Comparison with precipitation in other major Chinese cities. *Environ. Pollut.* **2009**, *157*, 35–41, doi:10.1016/j.envpol.2008.08.001.
29. Qiao, X.; Xiao, W.; Jaffe, D.; Kota, S.H.; Ying, Q.; Tang, Y. Atmospheric wet deposition of sulfur and nitrogen in Jiuzhaigou National Nature Reserve, Sichuan Province, China. *Sci. Total Environ.* **2015**, *511*, 28–36, doi:10.1016/j.scitotenv.2014.12.028.
30. US-EPA Positive Matrix Factorization Model 2018.
31. US-EPA EPA Positive Matrix Factorization (PMF) 5.0 - Fundamentals and User Guide. *Environ. Prot. Agency Off. Researc Dev. Publushing House Whashington, DC 20460* **2014**, 136.
32. Paatero, P. Least squares formulation of robust non-negative factor analysis. *Chemom. Intell. Lab. Syst.* **1997**, *37*, 23–35, doi:10.1016/S0169-7439(96)00044-5.
33. Paatero, P.; Tapper, U. Positive matrix factorization: A non-negative factor model with optimal utilization of error estimates of data values. *Environmetrics* **1994**, *5*, 111–126, doi:10.1002/env.3170050203.
34. Reff, A.; Eberly, S.I.; Bhave, P. V. Receptor modeling of ambient particulate matter data using positive matrix factorization: Review of existing methods. *J. Air Waste Manag. Assoc.* **2007**, *57*, 146–154, doi:10.1080/10473289.2007.10465319.
35. Alves, D.D.; Backes, E.; Rocha-Uriartt, L.; Riegel, R.P.; de Quevedo, D.M.; Schmitt, J.L.; da Costa, G.M.; Osório, D.M.M. Chemical composition of rainwater in the Sinos River Basin, Southern Brazil: a source apportionment study. *Environ. Sci. Pollut. Res.* **2018**, *25*, 24150–24161, doi:10.1007/s11356-018-2505-1.
36. Mehr, M.R.; Keshavarzi, B.; Sorooshian, A. Influence of natural and urban emissions on rainwater chemistry at a southwestern Iran coastal site. *Sci. Total Environ.* **2019**, *668*, 1213–1221, doi:10.1016/j.scitotenv.2019.03.082.
37. Prathibha, P.; Kothai, P.; Saradhi, I. V.; Pandit, G.G.; Puranik, V.D. Chemical characterization of precipitation at a coastal site in Trombay, Mumbai, India. *Environ. Monit. Assess.* **2010**, *168*, 45–53, doi:10.1007/s10661-009-1090-7.
38. Xu, H.; Bi, X.H.; Feng, Y.C.; Lin, F.M.; Jiao, L.; Hong, S.M.; Liu, W.G.; Zhang, X.-Y. Chemical composition of precipitation and its sources in Hangzhou, China. *Environ. Monit. Assess.* **2011**, *183*, 581–592, doi:10.1007/s10661-011-1963-4.

39. Meng, Y.; Zhao, Y.; Li, R.; Li, J.; Cui, L.; Kong, L.; Fu, H. Characterization of inorganic ions in rainwater in the megacity of Shanghai: Spatiotemporal variations and source apportionment. *Atmos. Res.* **2019**, *222*, 12–24, doi:10.1016/j.atmosres.2019.01.023.
40. Akpo, A.B.; Galy-Lacaux, C.; Laouali, D.; Delon, C.; Liousse, C.; Adon, M.; Gardrat, E.; Mariscal, A.; Darakpa, C. Precipitation chemistry and wet deposition in a remote wet savanna site in West Africa: Djougou (Benin). *Atmos. Environ.* **2015**, *115*, 110–123, doi:10.1016/j.atmosenv.2015.04.064.
41. Zhao, M.; Li, L.; Liu, Z.; Chen, B.; Huang, J.; Cai, J.; Deng, S. Chemical Composition and Sources of Rainwater Collected at a Semi-Rural Site in Ya'an, Southwestern China. *Atmos. Clim. Sci.* **2013**, *03*, 486–496, doi:10.4236/acs.2013.34051.
42. Seinfeld, J.H.; Pandis, S.N. *Atmospheric Chemistry and Physics: From Air Pollution to Climate Change*; 2nd ed.; John Wiley & Sons, Inc.: Hoboken, New Jersey, 1998; Vol. 51; ISBN 9780471720171.
43. Mimura, A.M.S.; Almeida, J.M.; Vaz, F.A.S.; de Oliveira, M.A.L.; Ferreira, C.C.M.; Silva, J.C.J. Chemical composition monitoring of tropical rainwater during an atypical dry year. *Atmos. Res.* **2016**, *169*, 391–399, doi:10.1016/j.atmosres.2015.11.001.
44. Bakayoko, A.; Galy-Lacaux, C.; Yoboué, V.; Hickman, J.E.; Roux, F.; Gardrat, E.; Julien, F.; Delon, C. Dominant contribution of nitrogen compounds in precipitation chemistry in the Lake Victoria catchment (East Africa). *Environ. Res. Lett.* **2021**, *16*, doi:10.1088/1748-9326/abe25c.
45. Migliavacca, D.; Teixeira, E.C.; Wiegand, F.; Machado, A.C.M.; Sanchez, J. Atmospheric precipitation and chemical composition of an urban site, Guaíba hydrographic basin, Brazil. *Atmos. Environ.* **2005**, *39*, 1829–1844, doi:10.1016/j.atmosenv.2004.12.005.
46. Xiao, J. Chemical composition and source identification of rainwater constituents at an urban site in Xi'an. *Environ. Earth Sci.* **2016**, *75*, 1–12, doi:10.1007/s12665-015-4997-z.
47. Tositti, L.; Pieri, L.; Brattich, E.; Parmeggiani, S.; Ventura, F. Chemical characteristics of atmospheric bulk deposition in a semi-rural area of the Po Valley (Italy). *J. Atmos. Chem.* **2018**, *75*, 97–121, doi:10.1007/s10874-017-9365-9.
48. Herrera, J.; Rodríguez, S.; Baéz, A.P. Chemical composition of bulk precipitation in the metropolitan area of Costa Rica, Central America. *Atmos. Res.* **2009**, *94*, 151–160, doi:10.1016/j.atmosres.2009.05.004.
49. Yatkin, S.; Adali, M.; Bayram, A. A study on the precipitation in Izmir, Turkey: chemical composition and source apportionment by receptor models. *J. Atmos. Chem.* **2016**, *73*, 241–259, doi:10.1007/s10874-015-9325-1.
50. Singh, S.P.; Khare, P.; Satsangi, G.S.; Lakhani, A.; Maharaj Kumari, K.; Srivastava, S.S. Rainwater composition at a regional representative site of a semi-arid region of India. *Water. Air. Soil Pollut.* **2001**, *127*, 93–108, doi:10.1023/A:1005295215338.
51. Zhang, M.; Wang, S.; Wu, F.; Yuan, X.; Zhang, Y. Chemical compositions of wet precipitation and anthropogenic influences at a developing urban site in southeastern China. *Atmos. Res.* **2007**, *84*, 311–322, doi:10.1016/j.atmosres.2006.09.003.
52. Zeng, J.; Han, G.; Wu, Q.; Tang, Y. Effects of agricultural alkaline substances on reducing the rainwater acidification: Insight from chemical compositions and calcium isotopes in a karst forests area. *Agric. Ecosyst. Environ.* **2020**, *290*, 106782, doi:10.1016/j.agee.2019.106782.
53. Guo, S.H.; Gao, P.; Wu, B.; Zhang, L.Y. Fluorine emission list of China's key industries and soil fluorine concentration estimation. *J. Appl. Ecol.* **2019**, doi:10.13287/j.1001-9332.201901.002.
54. Klumpp, A.; Domingos, M.; Klumpp, G. Assessment of the vegetation risk by fluoride emissions from fertiliser industries at Cubatao, Brazil. *Sci. Total Environ.* **1996**, *192*, 219–228, doi:10.1016/S0048-9697(96)05298-9.
55. Vieira-Filho, M.; Lehmann, C.; Fornaro, A. Influence of local sources and topography on air quality and rainwater composition in Cubatão and São Paulo, Brazil. *Atmos. Environ.* **2015**, *101*, 200–208, doi:10.1016/j.atmosenv.2014.11.025.
56. IBGE Aplicação de Fertilizantes Nitrogenados por Unidades da Federação Available online: https://sidra.ibge.gov.br/tabela/770 (accessed on Jun 5, 2021).

57. Almaraz, M.; Bai, E.; Wang, C.; Trousdell, J.; Conley, S.; Faloona, I.; Houlton, B.Z. Erratum: Agriculture is a major source of NOx pollution in California (Science Advances DOI: 10.1126/sciadv.aao3477). *Sci. Adv.* **2018**, *4*, 1–9, doi:10.1126/SCIADV.AAU2561.

58. Niu, H.; He, Y.; Zhu, G.; Xin, H.; Du, J.; Pu, T.; Lu, X.; Zhao, G. Environmental implications of the snow chemistry from Mt. Yulong, southeastern Tibetan Plateau. *Quat. Int.* **2013**, *313–314*, 168–178, doi:10.1016/j.quaint.2012.11.019.

59. Niu, Y.; Li, X.; Pu, J.; Huang, Z. Organic acids contribute to rainwater acidity at a rural site in eastern China. *Air Qual. Atmos. Heal.* **2018**, *11*, 459–469, doi:10.1007/s11869-018-0553-9.